Hindawi Publishing Corporation
EURASIP Journal on Wireless Communications and Networking
Volume 2009, Article ID 212783, 10 pages
doi:10.1155/2009/212783

Research Article

Cross-Layer Resource Scheduling for Video Traffic in the Downlink of OFDMA-Based Wireless 4G Networks

Feroz A. Bokhari,[1] Halim Yanikomeroglu,[1] William K. Wong,[2] and Mahmudur Rahman[1]

[1] *Broadband Communications and Wireless Systems Centre, Department of System and Computer Engineering, Carleton University, Ottawa, ON, Canada K1S 5B6*
[2] *Terrestrial Wireless Systems Branch, Communication Research Centre of Canada, 3701 Carling Avenue, P.O. Box 11490 Station H, Ottawa, ON, Canada K2H 8S2*

Correspondence should be addressed to Mahmudur Rahman, mmrahman@sce.carleton.ca

Received 27 June 2008; Accepted 30 December 2008

Recommended by Zhu Han

Designing scheduling algorithms at the medium access control (MAC) layer relies on a variety of parameters including quality of service (QoS) requirements, resource allocation mechanisms, and link qualities from the corresponding layers. In this paper, we present an efficient cross-layer scheduling scheme, namely, Adaptive Token Bank Fair Queuing (ATBFQ) algorithm, which is designed for packet scheduling and resource allocation in the downlink of OFDMA-based wireless 4G networks. This algorithm focuses on the mechanisms of efficiency and fairness in multiuser frequency-selective fading environments. We propose an adaptive method for ATBFQ parameter selection which integrates packet scheduling with resource mapping. The performance of the proposed scheme is compared to that of the round-robin (RR) and the score-based (SB) schedulers. It is observed from simulation results that the proposed scheme with adaptive parameter selection provides enhanced performance in terms of queuing delay, packet dropping rate, and cell-edge user performance, while the total sector throughput remains comparable. We further analyze and compare achieved fairness of the schemes in terms of different fairness indices available in literature.

1. Introduction

The approaching fourth-generation (4G) wireless communication systems, such as the Third-Generation Partnership Project's Long Term Evolution (3GPP LTE) [1] and the IEEE 802.16 standards family (e.g., [2]), are projected to provide a wide variety of new multimedia services, ranging from high quality voice to other high-data-rate wireless applications. Another notable 4G wireless effort is the WINNER project, which aims to develop an innovative concept in radio access in order to achieve high flexibility and scalability with respect to data rates and radio environments [3]. Concepts developed in the WINNER project are applicable to evolving 4G standards due to common system considerations such as orthogonal frequency-division multiple access- (OFDMA-) based air interface, and support of relays and multiple-antenna configurations.

Unlike wireline networks, wireless resources are scarce. The data-rate capacity that a radio-frequency channel can support is limited by Shannon's capacity law. Moreover, due to the time-varying nature of wireless channel, radio resource management, especially packet scheduling and resource allocation, is crucial for wireless networks. Traditionally, the research on packet scheduling has emphasized QoS and fairness issues, and opportunistic scheduling algorithms have focused on exploiting the time-varying nature of the wireless channels in order to maximize throughput. This segregation between packet scheduling and radio resource allocation is inefficient. As fairness and throughput are reciprocally related, an intelligent compromise is necessary to obtain the required QoS while exploiting the time-varying characteristics of the wireless channel. Therefore, it is important to merge the packet scheduling and the resource allocation to design a cross-layer scheduling scheme [4].

A number of scheduling schemes in the literature analyze physical- (PHY-) and MAC-related design issues by assuming that all users are backlogged, that is, all users in the system

have nonempty buffers. However, it is shown in [5] that this assumption is not always correct, since the number of packets in the buffers can vary significantly, and there is a relatively high probability that the buffers are empty. For example, in time-slotted networks, the packets in the queues are aggregated into time slots. Consequently, empty queues and partially filled time slots will affect the system performance. Furthermore, these non-queue-aware scheduling algorithms lack the capability to provide required fairness among user terminals (UTs). Hence, it becomes necessary to consider queue states in scheduling and resource allocation [6].

In recent years, some schemes have considered integrating packet scheduling and radio resource scheduling into queue and channel aware scheduling algorithms. In [7], a weighted fair queuing (WFQ) scheduling scheme is proposed, where the largest share of the radio resources is given to the users with the best instantaneous channel conditions in a code division multiplexing (CDM-) based network. Another example of a queue- and channel-aware scheduling algorithm is the modified-largest weighted delay first (M-LWDF) algorithm, where priorities are given to the users with maximum queuing delays weighted by their instantaneous and average rates [8]. The associated decision metrics in these schemes are based on the combination of the delay and instantaneous channel rates. Finding an optimal metric based on these parameters is difficult due to varying requirements for different service classes.

In this paper, we present a scheduler which comprises packet scheduling and resource mapping taking both queue and channel states into account. In the first level of scheduling (packet scheduling), users to be served are selected based on the token bank fair queuing (TBFQ) algorithm, considering fairness and delay constraints among users. Although TBFQ was originally proposed for single-carrier time-division multiple access (TDMA) systems [9], it has been modified in this study by introducing additional parameters that adaptively interact with the second level of scheduling (resource mapping). These parameters take into account the network loading and the user channel conditions. Based on these parameters, the second-level scheduler assigns resources to the selected users in an adaptive manner that exploits the frequency selectivity of the OFDMA air interface. The modified combined scheduling scheme is called ATBFQ.

The performance of ATBFQ is studied in the context of the WINNER wide-area downlink scenario and is compared to that of the SB scheduling algorithm (which was the baseline scheduling scheme in WINNER) [10] and the RR scheme by extensive simulations. The rest of this paper is organized as follows. In Section 2, the ATBFQ algorithm is described in detail, along with its parameter selection. Methods of fairness assessment are addressed in Section 3. The system model and the simulation parameters are presented in Section 4. Simulation results are provided in Section 5, followed by conclusions in Section 6.

2. ATBFQ Scheduling Algorithm

2.1. Original TBFQ Algorithm. The TBFQ algorithm was initially developed for wireless packet scheduling in the downlink of TDMA systems [9, 11], and was later modified for wireless multimedia services using uplink as well. Its concept was based on the leaky-bucket mechanism which polices flows and conforms them to a certain traffic profile.

A traffic flow belonging to user i is characterized by the following parameters:

λ_i: packet arrival rate,

r_i: token generation rate,

p_i: token pool size,

E_i: counter that keeps track of the number of tokens borrowed from or given to the token bank by flow i.

Each L-byte packet consumes L tokens. For each flow i, E_i is a counter that keeps track of the number of tokens borrowed from or given to the token bank. As tokens are generated at rate r_i, the tokens overflowing from the token pool (of size p_i bytes) are added to the token bank, and E_i is incremented by the same amount. When the token pool is depleted and there are still packets to be served, tokens are withdrawn from the bank by flow i, and E_i is decreased by the same amount. Thus, during periods when the incoming traffic rate of flow i is less than its token generation rate, the token pool always has enough tokens to serve arriving packets, and E_i increases and becomes positive and increasing. On the other hand, during periods when the incoming traffic rate of flow i is greater than its token generation rate, the token pool is emptied at a faster rate than it can be refilled with tokens. In this case, the connection may borrow tokens from the bank. The priority of a connection in borrowing tokens from the bank is determined by the priority index (P_i), given by

$$P_i = \frac{E_i}{r_i}. \tag{1}$$

By prioritizing in this manner, we ensure that flows belonging to UTs that are suffering from severe interference, and shadowing conditions in particular, will have a higher priority index, since they will contribute to the bank more often.

2.2. ATBFQ Algorithm. In this study, the TBFQ algorithm, originally proposed for single carrier TDMA systems, is improved by introducing adaptive parameter selection and extended to suit the WINNER multicarrier OFDMA systems [12]. The motivation behind this modification was to incorporate the design and performance requirements of the scheduler in 4G networks into the original scheme. In such networks, the utilization of the resources and hence the performance of the network can be enhanced by making use of the multiuser diversity provided by the multiple access scheme being used. Also, such networks support users with high mobility. Therefore, in order to make use of the

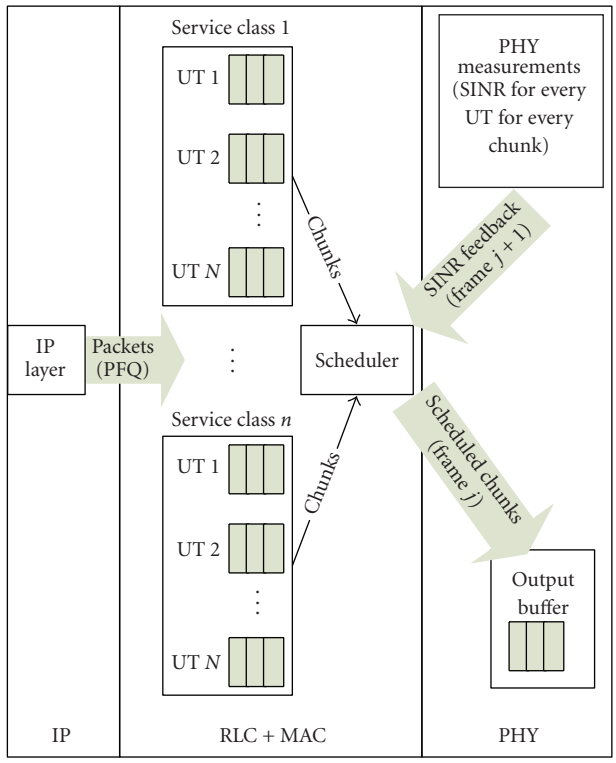

Figure 1: Overview of the proposed cross-layer scheduling operation.

channel feedback, faster scheduling (at a much smaller time scale) is required. Another requirement is the ability to maintain fairness and provide a minimum acceptable QoS performance to all users.

The basic time-frequency resource unit in OFDMA is denoted as a *chunk*. It consists of a rectangular time-frequency area that comprises a number of subsequent OFDM symbols and a number of adjacent subcarriers. Packets from the traffic flows are exclusively mapped on to these chunks based on QoS requirements obtained from the higher radio link control (RLC) layer along with the channel feedback received from the physical layer. The channel feedback comprises signal-to-interference plus noise ratio (SINR) which is measured in the downlink portion of the frame j at the UTs, as shown in Figure 1. This feedback is then provided to the BS in the uplink duration of the frame $j+1$ and can be utilized for scheduling purposes at the MAC layer in the downlink of the next frame, $j+2$. The frame duration, as mentioned in WINNER [13], is 0.6912 milliseconds. The feedback is valid for two frame durations, which is less than the coherence time for mobile speeds of up to 100 km/hr.

Like TBFQ, the ATBFQ scheduling principle is based on the leaky-bucket mechanism. Each traffic flow i is characterized by a packet arrival rate λ_i, token generation rate r_i, token pool size p_i, and a counter E_i to keep track of the number of tokens borrowed from or given to the token bank. Each L-byte packet consumes L tokens. As tokens are generated at rate r_i, the tokens overflowing from the token pool are added to the token bank, and E_i is incremented by the same amount. When the token pool is depleted and there are still packets to be served, tokens are withdrawn from the bank by flow i, and E_i is decremented by the same amount. A debt limit d_i is set as a threshold to limit the amount a UT can borrow from the bank. It also acts as a measure to prevent malicious UTs (transmitting at unusually high transmission rates) from borrowing extensively. The packets are then queued in subqueues in a per-flow queuing (PFQ) manner such that each subqueue belongs to a particular flow, as shown in Figure 1.

The operation of the ATBFQ scheduler is shown by the flowchart shown in Figure 2. This can be summarized by the following steps, which are executed each time the scheduler is invoked at the beginning of the frame.

Step 1. At the scheduler, information is retrieved from the higher layer about all active users using the *getActiveUsers()* function. An active user is defined as a backlogged queue which has packets waiting to be served.

Step 2. Based on this list of active users, a priority is calculated according to the index given by (1). The *highestBorrowPriority()* function is called to calculate this for all active users N_{act}. This function then returns the user i with the highest priority given by

$$i^*(t_k) = \underset{1\le i\le N_{\text{act}}}{\arg\max}(P_i). \tag{2}$$

Step 3. Using the *borrowbudget()* function, a certain budget is calculated for the priority user i^* which depends on the token counter E_i^*, and the debt limit d_i^*, and is given by $E_i^* - d_i^*$. E_i^* keeps track of how much the user has borrowed or given to the bank. The debt limit d_i^* keeps track of how much a user can further borrow from the bank in order to accommodate the burstiness of the traffic over the long term.

Step 4. If the calculated budget is less than the bank size, resources are allocated to the user i using the *maxSINR()* function. This is the second level of scheduling, and deals with allocation of chunk resources to the selected user i. This allocation is based on the maximum SINR principle, where the chunk j with the best SINR is given to the selected user [14] and can be expressed by

$$j^*(t_k) = \underset{1\le j\le N_{\text{chunks}}}{\arg\max}\,(\gamma_{ij}(t_k)), \tag{3}$$

where γ_{ij} is the SINR of the selected user i in chunk j. This is the most opportunistic of all scheduling algorithms for time-slotted networks. This means that the adaptive modulation and coding (AMC) policy maximally exploits the frequency diversity of the time-frequency resource, where a chunk is allocated to only one user and a user can have multiple chunks in a scheduling instant.

Step 5. The *resourceMap()* function determines the amount of bits that can be mapped to the chunk depending on the AMC mode used.

Step 6. Each time a chunk resource is allocated, the *updateCounter()* function is called. This function updates the bank, the counter E_i, and the allocated budget.

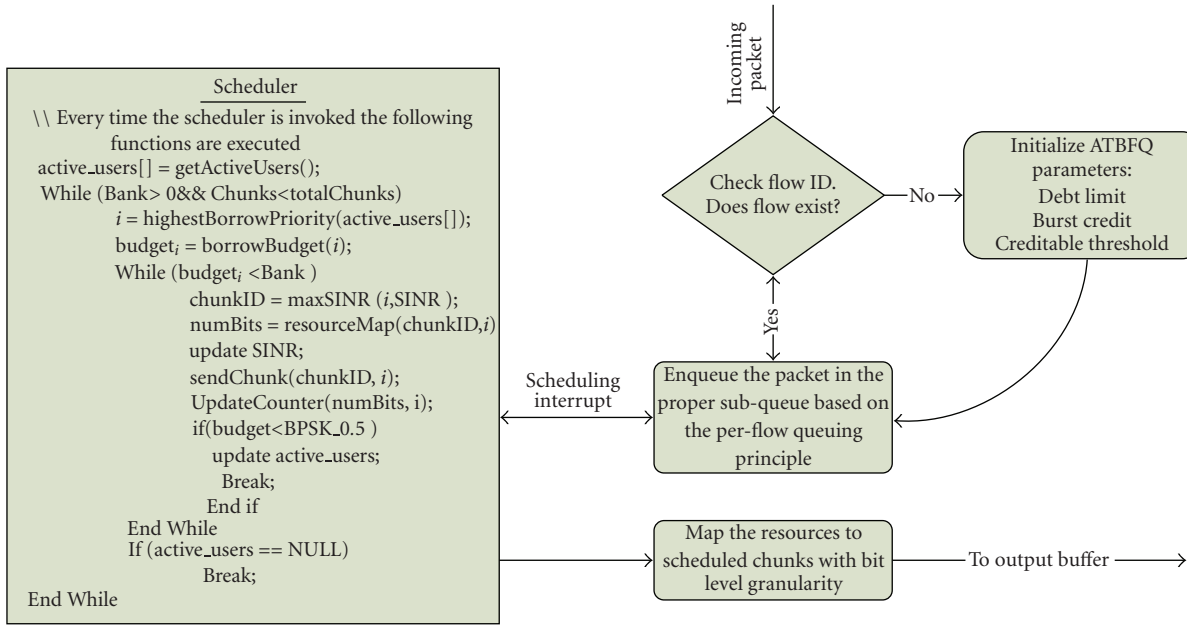

Figure 2: Flowchart of scheduling operation.

The selected user i gets to transmit as long as (1) its queue remains backlogged and (2) the allocated budget is less than the total bank size and more than the number of bits that can be supported with the lowest AMC mode (binary phase-shift keying (BPSK) rate-1/2, considered in this study). If either of these conditions is not satisfied, the user is classified as nonactive. A new priority is calculated on the updated active users, and Steps 1–6 are repeated. This procedure is repeated until there are no chunk resources available or there are no active users.

2.3. ATBFQ Parameter Selection. The performance of the ATBFQ scheduler depends on its parameters that define the debt limit, the burst credit (BC), and the token generation rate. The token generation rate is critical to the extent to which the burstiness of the UT traffic can be accommodated. A UT in its burst mode transmits more data in a short interval of time than its actual statistics, and hence, requires more resources in order to maintain a certain QoS level. The debt limit is set to -5 MB. The token generation rate should be large enough to handle instantaneous bursty traffic. In simulations, this generation rate has been considered three times larger than the average packet arrival rate.

The burst credit for flow i (BC_i) determines the amount of bits selected user i^* can receive in a frame. While this quantity was a fixed value in TBFQ, it is adaptive in ATBFQ. In a cellular network, the user loading level in terms of active users per sector is highly dynamic, due to the ON and OFF characteristics of the bursty traffic. It is observed through simulations that for low-loading cases, a higher value for BC_i performs better, as shown in Table 1. On the other hand, for high-loading conditions, a lower value for BC_i is desired as it exploits multiuser diversity, as shown in Table 2. It is further seen that for both low- and high-loading conditions, BC_i should be adapted per user basis in order to obtain high spectral efficiency. For UT i, this adaptive value can be formulated as

$$\mathrm{BC}_i = \frac{\eta_i(\mathrm{bits/sec/Hz}) \times M(\mathrm{Hz}\cdot\ \mathrm{sec}) \times N_{\mathrm{chunks}}}{N_{\mathrm{act}}}, \quad (4)$$

where η_i is the past spectral efficiency, N_{chunks} is the number of available chunks, M is the amount of time-frequency resources in a chunk, and N_{act} is the number of active UTs in that particular scheduling frame. η_i is a moving average which is updated each time by averaging over the past 100 transmissions of user i.

3. Fairness Study

Opportunistic scheduling algorithms aim to provide high throughput for UTs having good channel conditions (closer to the BS), and consequently, experience a degraded performance. In such cases, the overall throughput of the system is maximized but the fairness amongst UTs is greatly affected. Therefore, it is essential to design a performance metric that is an appropriate indicator of the fairness. One such index is the *Jain's fairness index* proposed in [15]. This fairness index is bounded between zero and unity, and has been widely used [16, 17]. If a system allocates resources to n contending UTs such that the ith user receives an allocation x_i, then this fairness index $f_I(x)$ is given by

$$f_I(x) = \frac{\left[\sum_{i=1}^{n} x_i\right]^2}{n\sum_{i=1}^{n} x_i^2}, \quad (5)$$

where $x_i \geq 0$. This index measures the equality of UT allocation x. If x_is are equal for all UTs, then the fairness index is 1 and the system is 100% fair, and vice versa. In this

Table 1: Burst credit for ATBFQ for low loading (8 users).

Burst credit (BC)	Queuing delay (sec)	Packets dropped (per frame)	Throughput (Byte per frame)	Spectral efficiency (bits/sec/Hz)
BC = 1000	0.025	4.36	815.4	2.37
BC = 5000	0.017	0.76	1473.3	2.05
BC = 10000	0.015	0.42	1546.6	1.98
Adaptive BC	0.012	0.30	1551.1	2.34

Table 2: Burst credit for ATBFQ for high loading (20 users).

Burst credit (BC)	Queuing delay (sec)	Packets dropped (per frame)	Throughput (Byte per frame)	Spectral efficiency (bits/sec/Hz)
BC = 1000	0.044	3.19	2299.4	2.09
BC = 5000	0.036	3.98	2094.0	1.88
BC = 10000	0.033	4.00	2090.4	1.87
Adaptive BC	0.038	2.01	2497.1	2.29

paper, the allocation metric "x" is defined as the ratio of UT throughput and queue size, and is given by

$$x_i = \frac{TP_i^{(t_1,t_2)}}{Q_i^{(t_1,t_2)}}, \tag{6}$$

where $TP_i^{(t_1,t_2)}$ is the transmitted throughput in bits for UT i during the time interval $[t_1, t_2]$ and $Q_i^{(t_1,t_2)}$ is the total number of packets arriving in the queue for UT i during (t_1, t_2). In simulations, (t_1, t_2) is chosen to be equal to 16 frame time durations.

In (6), the throughput is normalized to avoid ambiguity since the throughput alone as a metric does not provide an insight into the overall fairness.

Another method of fairness assessment, proposed in WiMAX standard [18], is determined by the normalized cumulative distributive function (CDF) of throughput per UT. The normalized UT throughput with respect to the average throughput, $\widetilde{T}_i$ for UT i, is expressed by

$$\widetilde{T}_i = \frac{T_i}{(1/n)\sum_{j=1}^{n} T_j}, \tag{7}$$

where T_i is the instantaneous throughput of UT i in a particular frame, and n is the total number of UTs. As stated in [18], the CDF of this normalized throughput should lie to the right of the coordinates (0.1, 0.1), (0.2, 0.2), and (0.5, 0.5).

The results using both of these fairness assessment methods are discussed in detail in Section 5.

4. System Model and Simulation Parameters

ATBFQ is studied in the wide-area downlink scenario. To reduce the simulation complexity, the bandwidth is reduced to 15 MHz from the original 45 MHz. The chunk dimension is given as 8 subcarriers by 12 OFDM symbols or 312.5 kHz × 345.6 microseconds. The frame duration is defined as 691.2 microseconds, that is, there are a total of 96 chunks per frame.

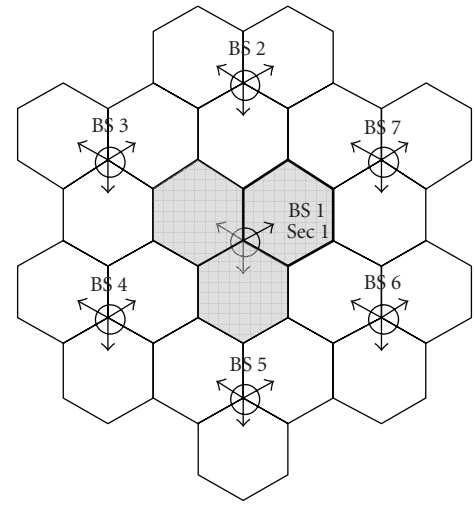

Figure 3: Network layout.

The network layout under investigation is shown in Figure 3. Each cell in the network has three sectors. A frequency reuse factor of 1 in each sector (all resources are used in each sector) is assumed. The UTs are uniformly placed in the central sector.

Time- and frequency-correlated Rayleigh channel samples obtained from power delay profile for the WINNER wide area scenario are used to generate the channel fading. The user speed is defined as 70 km/hr, and the intersite distance is 1 km. The following exponential path-loss model has been used [19]

$$\mathrm{PL} = 38.4 + 35.0 \log_{10}(d)[\mathrm{dB}], \tag{8}$$

where PL is the path loss in dB, and d is the transmitter-receiver separation in meters.

The average thermal noise power is calculated with a noise figure of 7 dB. We have considered independent lognormal random variables with a standard deviation of

8 dB for shadowing. Sector transmit power is assumed to be 46 dBm, and chunks are assigned fixed equal powers.

The interference is modeled by considering the effect of intercell interference and intracell interference on the sector of interest in the central cell (denoted as sector 1 in BS 1). For this purpose, the interference from the first tier is taken into account. In this case, for a link of interest in sector 1 in BS 1, the interference will comprise 18 (6 BS $\times$ 3 sectors) intercell and 2 intracell links.

The SINR obtained for chunk j of user i can be expressed by

$$\mathrm{SINR}_{i,j} = \frac{P^{1,1}_{\mathrm{signal}\,i,j}}{(P_{\mathrm{inter}\,i,j} + P_{\mathrm{intra}\,i,j}) + P_{\mathrm{noise}\,i,j}}, \tag{9}$$

where $P^{1,1}_{\mathrm{signal}\,i,j}$ denotes the desired signal power in sector 1 in BS 1, and $P_{\mathrm{noise},i}$ is the noise power. For the given layout in Figure 3, intracell interference $P_{\mathrm{intra},i,j}$, and intercell interference $P_{\mathrm{inter},i,j}$ are given by the following expressions:

$$\begin{aligned} P_{\mathrm{intra}\,i,j} &= \sum_{s=2}^{3} I_j^{b=1,s} X_I, \\ P_{\mathrm{inter}\,i,j} &= \sum_{b=2}^{7} \sum_{s=1}^{3} I_j^{b,s} X_I, \end{aligned} \tag{10}$$

where $I_j^{b,s}$ is the interference power for chunk j from sector s in BS b. X_I has a binary value defined by

$$X_I = \begin{cases} 1, & x \le \mathrm{AF}, \\ 0, & x > \mathrm{AF}, \end{cases} \tag{11}$$

where x is a uniform random variable defined over $[0, 1]$, and AF (activity factor) is defined as a probability for a particular interfering link to be active. For example, AF of 1 denotes a high level of interference where all the links are active interferers (100% interference).

Adaptive modulation with block low-density parity-check (B-LDPC) code is used. Thresholds for transmission schemes are determined assuming a block length of 1704 bits and 10% block error rate (BLER) as shown in Table 3 [13]. A chunk using quadrature phase-shift queueing (QPSK) rate-1/2 can carry 96 information bits. This is based on the initial transmissions, that is, hybrid automatic repeat request (HARQ) retransmissions are not considered. Real-time video streaming traffic is used in this study. Two interrupted renewal process (IRP) sources are superimposed to model user's video traffic in the downlink transmission as indicated in [20]. The average packet rate of one UT is 1263.8 packets per second. The resulting downlink data rate for each user is 1.92 Mbps.

The performance of the ATBFQ algorithm is compared to that of the RR and the SB algorithms. The SB algorithm was proposed in [10], and was modified to the WINNER multicarrier OFDMA system for this work. It is a variation of the proportional fair (PF) algorithm which is the most widely adopted opportunistic scheduling algorithm [21]. The SB scheduler selects user i in slot k with the best score,

Table 3: Lookup table for AMC modes and corresponding chunk throughput.

AMC mode	SINR (dB)	Chunk throughput (bits)
BPSK 1/2	$0.2311 \ge \mathrm{SINR} > -1.7$	48
BPSK 2/3	$1.231 \ge \mathrm{SINR} > 0.231$	72
QPSK 1/2	$3.245 \ge \mathrm{SINR} > 1.231$	96
QPSK 2/3	$4.242 \ge \mathrm{SINR} > 3.245$	128
QPSK 3/4	$6.686 \ge \mathrm{SINR} > 4.242$	144
16QAM 1/2	$9.079 \ge \mathrm{SINR} > 6.686$	192
16QAM 2/3	$10.33 \ge \mathrm{SINR} > 9.079$	256
16QAM 3/4	$14.08 \ge \mathrm{SINR} > 10.33$	288
64QAM 2/3	$15.6 \ge \mathrm{SINR} > 14.08$	384
64QAM 3/4	$\mathrm{SINR} > 15.6$	432

where the score is calculated based on the current rank of the user's SINR among its past values in the current window $\{\gamma_i(t_k), \gamma_i(t_{k-1}), \ldots, \gamma_i(t_{k-W+1})\}$, where $\gamma_i(t_k)$ is the SINR value of a user at time instant k, and W is the window size. The corresponding score for the user i is given by

$$s_i(t_k) = 1 + \sum_{l=1}^{W-1} 1_{\{r_i(t_k) < r_i(t_{k-l})\}} + \sum_{l=1}^{W-1} 1_{\{r_i(t_k) = r_i(t_{k-l})\}} X_l, \tag{12}$$

where X_l are i.i.d. random variables on $\{0, 1\}$ with $P_r(x = 0) = P_r(x = 1) = 0.5$.

Packets are scheduled on a frame-by-frame basis at the start of every frame. Any packet that arrives at current frame time will have to wait at least until the start of the next frame. As video streaming has the most stringent delay requirement, packets are dropped if they experience a delay in excess of 190 milliseconds. The simulation parameters are summarized in Table 4; most of them are taken from the WINNER baseline simulation assumptions [13].

5. Simulation Results

The performance results are classified into four categories: (1) average user statistics, (2) performance of the cell-edge users, (3) effect of varying user loading and interference conditions, and (4) fairness analysis. Furthermore, the results are compared to the SB and RR algorithms. The window size plays an important role in the performance of the SB algorithm [10]. The performance of ATBFQ has been studied with different window sizes in the WINNER context [22, 23].

5.1. User Performance. Figure 4 shows the CDF of the packets dropped per frame for low and high loading, respectively. These curves indicate the opportunistic nature of SB, since it tends to favor the users with good channel conditions. Consequently, a higher drop rate, even at low loading, is observed for SB.

The CDF of average user throughput per sector (measured in bytes per frame) for 8 and 20 user loading cases is shown in Figure 5. ATBFQ performs better for the

Table 4: Summary of simulation parameters.

Parameter	Used value/model
Scenario	Wide area DL (frequency adaptive)
Channel model	WINNER C2 channel
Shadowing	Independent lognormal random variables (standard deviation 8 dB)
Sector Tx antenna	120° directional with WINNER baseline antenna pattern
UT receive antenna	Omnidirectional
Intersite distance	1000 m
Signal bandwidth	15 MHz (i.e., 48 chunks which is 1/3rd of the baseline assumptions)
Mobility	70 km/hr
Sector Tx power	46 dBm
Scheduler	Adaptive Token Bank Fair Queuing, score based, and round-robin
Interference model	brute force method (central cell is considered with interference from the 1st-tier)
Antenna configuration	Single-in-single-out (SISO)
Coding	B-LDPCC
AMC modes	BPSK (rate 1/2 and 2/3), QPSK (rate 1/2, 2/3, and 3/4), 16QAM (rate 1/2, 2/3, and 3/4), and 64QAM (rate 2/3 and 3/4)
AMC thresholds	With FEC block of 1728 bits and 10% BLER
Frame duration	0.6912 ms (scheduling interval)
Traffic model	1.9 Mbps 2IRP model for MPEG video
Packet size	188 Bytes
Packet drop criterion	Delay ≥ 0.19 sec
Simulation time	60 sec
Simulation tools	MATLAB and OPNET

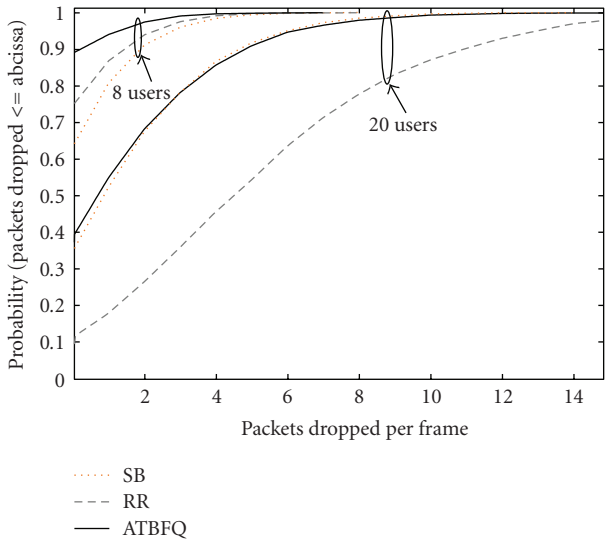

Figure 4: CDF of packets dropped per user per frame.

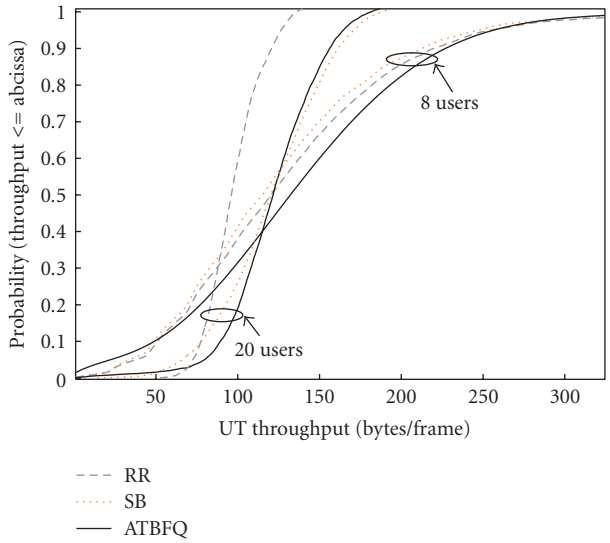

Figure 5: CDF of user throughput.

lower loading case, whereas SB achieves marginally higher throughput at higher loading. For the high loading case, it is observed that the CDF curve for ATBFQ has a steeper slope indicating better fairness, since users are served with similar throughput. Note that this is not true for SB. As ATBFQ attempts to maintain fairness, it tries to serve cell-edge users with poor channel conditions as compared to those located closer to the BS. Therefore, ATBFQ also utilizes more chunks. On the other hand, SB aims to maximize the throughput while being fair in the opportunistic sense.

5.2. Cell-Edge User Performance. Figure 6 shows the packet transmit ratio (defined as the transmitted packet per total packets generated) versus distance from BS for 20 users per sector. It can be observed that as the distance increases, the packet transmit ratio for SB decreases, that is, the number of

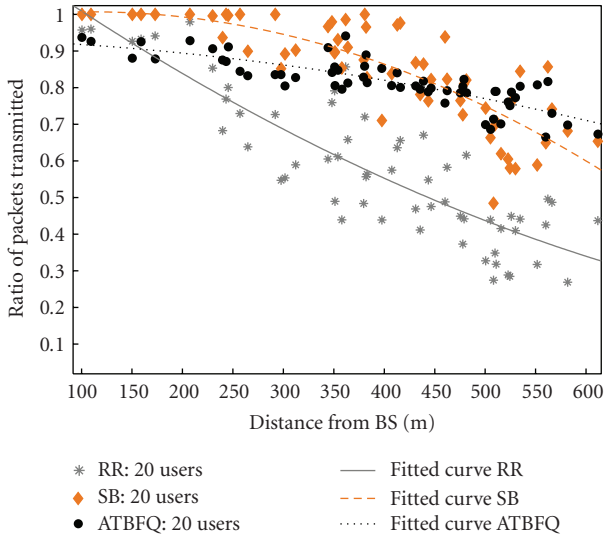

Figure 6: Ratio of packets dropped versus distance form BS.

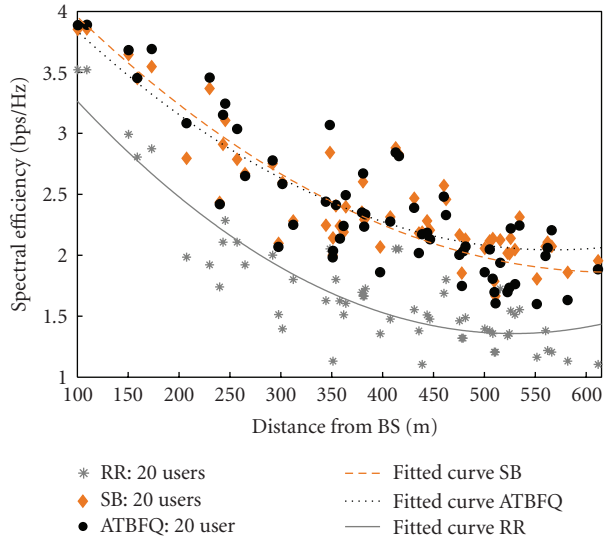

Figure 7: Average user spectral efficiency versus distance form BS.

dropped packets increases. This can be further visualized by the quadratic-fitted curves for both algorithms, which show their respective trends with the varying distance. As SB tries to maximize the throughput, the cell-edge users are affected, and suffer packet losses. ATBFQ, on the other hand, is fair in nature and shows enhanced performance for the cell-edge users. If a cell-edge user is suffering from poor channel conditions, ATBFQ gives it priority to transmit in the next scheduling interval. By assigning priorities in such a manner, ATBFQ considerably improves the spectral efficiency for the cell-edge users, as shown in Figure 7.

5.3. Varying User Loading and Interference Conditions. Performance indicators such as average dropped packets, average UT throughput, and average UT queuing delay have been considered in evaluating ATBFQ by comparison with the reference SB and RR schemes.

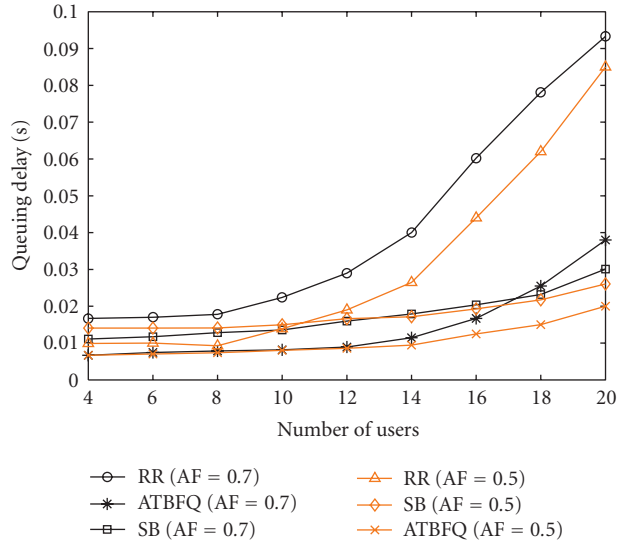

Figure 8: Average UT queuing delay versus number of UTs.

Figures 8, 9, and 10 show the performance results for average UT queuing delay, average packets dropped per frame, and the total sector throughput, respectively, in varying loading conditions for ATBFQ, SB, and RR. The curves are plotted for two different AFs of 0.5 and 0.7 to model moderate and high interference situations, respectively. ATBFQ outperforms the reference SB and RR algorithms in terms of the above-mentioned performance parameters for all loading conditions when the AF is 0.5. In this case, the UTs experience better channel conditions resulting from low interference. Hence, fewer chunks are utilized to transmit data as compared to the number of chunks utilized for a higher AF. Consequently, RR performs better than SB at lower loading levels.

For low-to-medium loading with an AF of 0.7, it is observed again that ATBFQ outperforms the reference schemes in terms of all observed parameters. This trend changes as network loading increases to 20 UTs per sector. In this case, SB outperforms ATBFQ and RR in terms of average UT queuing delay, average packets dropped per frame, and the total sector throughput, respectively. This is due to the fact that SB is opportunistic in nature, whereas ATBFQ is fairness aware. As the number of UTs increases, SB takes advantage of the multiuser diversity to achieve higher throughput.

5.4. Fairness Analysis. The CDF of the Jain's fairness index given by (5) is shown in Figure 11. These curves represent network loading of 20 UTs per sector with an AF of 0.7. It is observed that ATBFQ achieves better fairness compared to SB and RR. Figure 12 shows the CDF plot of the normalized throughput given by (7) for 20 UTs per sector with an AF of 0.7. By normalizing the throughput, the performance of the cell edge users represented by the tail of the throughput CDF curve is enhanced. It is again observed that a higher

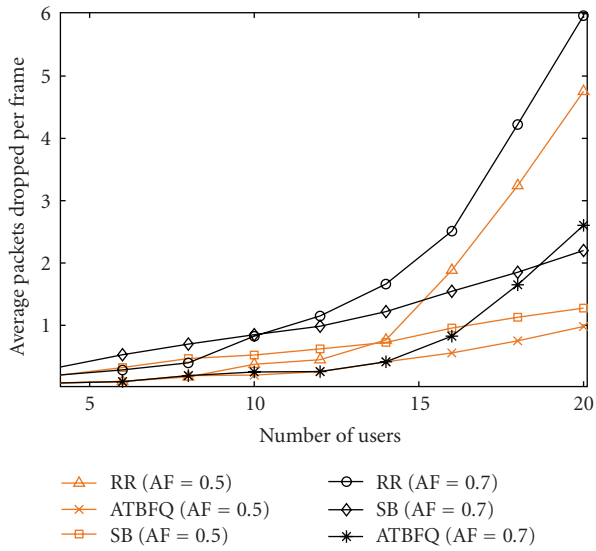

Figure 9: Average UT packets dropped per frame versus number of UTs.

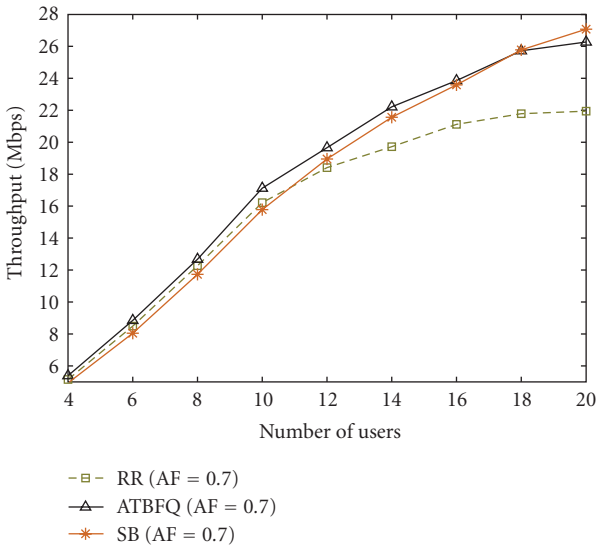

Figure 10: Sector throughput.

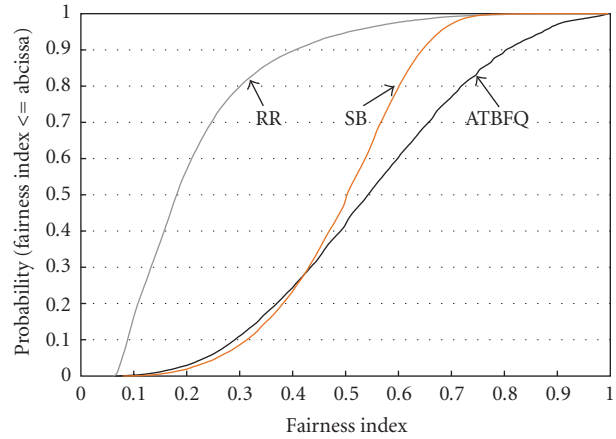

Figure 11: CDF of fairness index.

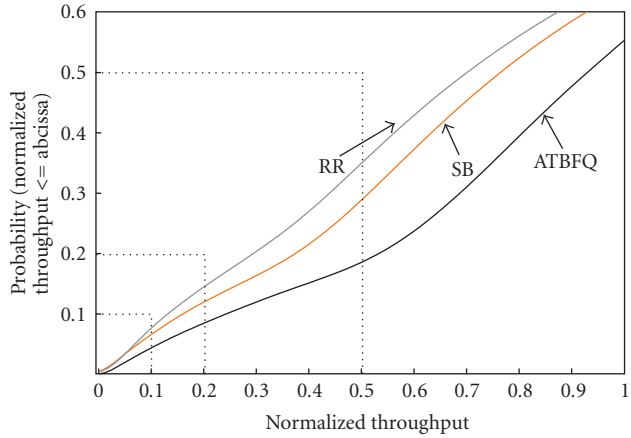

Figure 12: CDF of normalized throughput (zoomed in).

normalized throughput is achieved for ATBFQ compared to that in SB, and the curve lies to the right of the above-mentioned coordinates.

6. Conclusion

In this paper, the performance of the ATBFQ scheduling algorithm with adaptive parameter selection is investigated in the context of the 4G WINNER wide-area downlink scenario. It is a queue- and channel-aware scheduling algorithm which attempts to maintain fairness among all users. Performance of ATBFQ is presented with reference to the SB and RR schedulers. Being an opportunistic scheduler belonging to the proportional fair class, SB aims to maximize throughput by making use of multiuser diversity while trying to maintain fairness. However, this comes at a certain cost, since the cell edge users in this scheme, suffering from poor channel conditions, are more severely affected. Also, due to the bursty nature of the traffic, such users experience higher queueing delays, resulting in a higher number of packet dropping.

Contrary to SB, ATBFQ is a credit-based scheme which aims to accommodate the burstiness of the users by assigning them more resources in the short term, provided that long-term fairness is maintained. For lower to medium loading, ATBFQ provides higher throughput, lower queuing delay, and a lower number of packets dropped as compared to SB and RR. At high loading, ATBFQ still outperforms SB and RR with regard to the queuing delay and packet dropping, however, with a slight degradation in the sector throughput. This is because ATBFQ attempts to satisfy users with poor channel conditions by assigning more resources, even with a lower chunk spectral efficiency. An overall improvement of the performance of cell-edge users is observed in terms of spectral efficiency and packet-dropping ratio for ATBFQ as compared to SB and RR.

The observed throughput, queuing delay, and packet dropping rate clearly indicate the superiority of the ATBFQ

algorithm. This apparent improvement in the fairness performance of the ATBFQ algorithm based on these performance parameters is further validated by evaluating the fairness indices available in the literature.

Acknowledgments

The authors would like to express their gratitude to Mr. Jiangxin Hu for his technical support and Dr. Abdulkareem Adinoyi for providing his valuable comments on the manuscript. They also thank OPNET Technologies, Inc. for providing software license to carry out the simulations of this research. This work was a part of the Wireless World Initiative New Radio (WINNER) project, http://www.ist-winner.org/, with the support of the Natural Sciences and Engineering Research Council (NSERC) of Canada. Preliminary results of this work have been presented in IEEE VTC2008-Spring and IEEE VTC2008-Fall conferences.

References

[1] Overall Description: Stage 2 (Release 8), "3GPP Std. 3GPP E-UTRA and E-UTRAN Technical Specification TS 36.300 V8.4.0," March 2008, http://www.3gpp.org/ftp/Specs/html-info/36300.htm.

[2] IEEE 802.16 Std. 802.16j/D5, "Part 16: Air Interface for Fixed and Mobile Broadband Wireless Access Systems—Multihop Relay Specification," June 2008, http://www.ieee802.org/16.

[3] "Project Presentation," WINNER Deliverable D8.1, March 2004, http://www.ist-winner.org/deliverables_older.html.

[4] Q. Liu, X. Wang, and G. B. Giannakis, "A cross-layer scheduling algorithm with QoS support in wireless networks," *IEEE Transactions on Vehicular Technology*, vol. 55, no. 3, pp. 839–847, 2006.

[5] S. Borst, "User-level performance of channel-aware scheduling algorithms in wireless data networks," in *Proceedings of the 22nd Annual Joint Conference of the IEEE Computer and Communications Societies (INFOCOM '03)*, vol. 1, pp. 321–331, San Francisco, Calif, USA, March-April 2003.

[6] D. Wu and R. Negi, "Effective capacity: a wireless link model for support of quality of service," *IEEE Transactions on Wireless Communications*, vol. 2, no. 4, pp. 630–643, 2003.

[7] A. Stamoulis, N. D. Sidiropoulos, and G. B. Giannakis, "Time-varying fair queueing scheduling for multicode CDMA based on dynamic programming," *IEEE Transactions on Wireless Communications*, vol. 3, no. 2, pp. 512–523, 2004.

[8] M. Andrews, K. Kumaran, K. Ramanan, A. Stolyar, P. Whiting, and R. Vijayakumar, "Providing quality of service over a shared wireless link," *IEEE Communications Magazine*, vol. 39, no. 2, pp. 150–154, 2001.

[9] W. K. Wong and V. C. M. Leung, "Scheduling for integrated services in next generation packet broadcast networks," in *Proceedings of the IEEE Wireless Communications and Networking Conference (WCNC '99)*, vol. 3, pp. 1278–1282, New Orleans, La, USA, September 1999.

[10] T. Bonald, "A score-based opportunistic scheduler for fading radio channels," in *Proceedings of the 5th European Wireless Conference (EW '04)*, Barcelona, Spain, February 2004.

[11] W. K. Wong, H. Y. Tang, and V. C. M. Leung, "Token bank fair queuing: a new scheduling algorithm for wireless multimedia services," *International Journal of Communication Systems*, vol. 17, no. 6, pp. 591–614, 2004.

[12] "Final Report on Identified RI Key Technologies, System Concept, and their Assessment," WINNER I Deliverable D2.10, November 2005, http://www.ist-winner.org/deliverables_older.html.

[13] "Test Scenarios and Calibration Cases Issue 2," WINNER II Deliverable D6.13.7, December 2006, http://www.ist-winner.org/ deliverables.html.

[14] R. Knopp and P. A. Humblet, "Information capacity and power control in single-cell multiuser communications," in *Proceedings of IEEE International Conference on Communications (ICC '95)*, vol. 1, pp. 331–335, Seattle, Wash, USA, June 1995.

[15] R. Jain, D. Chiu, and W. Hawe, "A quantitative measure of fairness and discrimination for resource allocation in shared computer systems," Tech. Rep. DEC-TR-301, Digital Equipment Corporation, Maynard, Mass, USA, September 1984.

[16] H. Sirisena, A. Haider, M. Hassan, and K. Fawlikowski, "Transient fairness of optimized end-to-end window control," in *Proceedings of IEEE Global Telecommunications Conference (GLOBECOM '03)*, vol. 7, pp. 3979–3983, San Francisco, Calif, USA, December 2003.

[17] G. Berger-Sabbate, A. Duda, O. Gaudoin, M. Heusse, and F. Rousseau, "Fairness and its impact on delay in 802.11 networks," in *Proceedings of IEEE Global Telecommunications Conference (GLOBECOM '04)*, vol. 5, pp. 2967–2973, Dallas, Tex, USA, November-December 2004.

[18] IEEE 802.16 Std., "IEEE 802.16m Evaluation Methodology Document," September 2007, http://www.ieee802.org/16.

[19] "Final report on link level and system level channel models," WINNER I Deliverable D5.4, November 2005, http://www.ist-winner.org/deliverables_older.html.

[20] "Traffic model for 802.16 TG3 MAC/PHY simulations," IEEE 802.16 Work-in-progress document 802.16.3c-01/30r1, March 2001, http://www.ieee802.org/16.

[21] E. F. Chaponniere, P. J. Black, J. M. Holtzman, and D. N. C. Tse, "Transmitter directed code division multiple access system using path diversity to equitably maximize throughput," US Patent no. 6449490, September 2002.

[22] "Inteference Avoidance Concepts," WINNER II Deliverable D4.7.2, June 2007, http://www.ist-winner.org/deliverables.html.

[23] F. A. Bokhari, W. K. Wong, and H. Yanikomeroglu, "Adaptive token bank fair queuing scheduling in the downlink of 4G wireless multicarrier networks," in *Proceedings of the 67th IEEE Vehicular Technology Conference (VTC '08)*, pp. 1995–2000, Marina Bay, Singapore, May 2008.

EURASIP Journal on Advances in Signal Processing

Special Issue on Image Processing and Analysis in Biomechanics

Call for Papers

Computational methodologies of signal processing and analysis based on 1D-4D data are commonly used in different applications in society. In particular, image processing and analysis methodologies have enjoyed increased deployment in automated recognition, human-machine interfaces, computer-aided diagnostics, robotics surgery, and biomechanics analysis.

Image processing and analysis is fundamentally a multidisciplinary area, combining elements of informatics, mathematics, statistics, psychology, mechanics and physics, among others. One of the more important applications of image processing and analysis can be found in medical imagery, which continually promotes new research and development. Present trends include using statistical or physical procedures on medical images in order to have different objectives, such as organ segmentation, shape reconstruction, motion and deformation analysis, organ registration and comparison, virtual reality, computer-assisted therapy, or biomechanic analysis and simulation.

The research related with analysis and simulation of biomechanical structures has been a source of many challenging problems, involving geometric modeling, numerical modeling, biomechanics, material models for living tissues, experimental methodologies, and mechanobiology, as well as their application in clinical environments. A critical component for true realistic biomechanical analysis and simulations is to obtain accurately, from images, the geometric data and the behavior of the desired structures. For that, the use of automatic, efficient, and robust techniques of image processing and analysis is required.

The main objective of this Special Issue on *Image Processing and Analysis in Biomechanics* is to bring together recent advances in the field. Topics of interest include, but are not limited to:

- Signal processing in biomechanical applications
- Data interpolation, registration, acquisition and compression in biomechanics
- Segmentation of objects in images for biomechanical applications
- 3D reconstruction of objects from images for biomechanical applications
- 2D/3D tracking and object analysis in images for biomechanical applications
- 3D vision in biomechanics
- Biomechanical applications involving image processing and analysis algorithms
- Virtual reality in biomechanics
- Software development for image processing and analysis in biomechanics

Before submission authors should carefully read over the journal's Author Guidelines, which are located at http://www.hindawi.com/journals/asp/guidelines.html. Authors should follow the EURASIP Journal on Advances in Signal Processing manuscript format described at the journal site http://www.hindawi.com/journals/asp/. Prospective authors should submit an electronic copy of their complete manuscript through the journal Manuscript Tracking System at http://mts.hindawi.com/, according to the following timetable:

Manuscript Due	May 1, 2009
First Round of Reviews	August 1, 2009
Publication Date	November 1, 2009

Lead Guest Editor

João Manuel R. S. Tavares, Department of Mechanical Engineering and Industrial Management, Faculty of Engineering, University of Porto, Rua Dr. Roberto Frias, 4200-465 Porto, Portugal; tavares@fe.up.pt

Guest Editor

R. M. Natal Jorge, Department of Mechanical Engineering and Industrial Management, Faculty of Engineering, University of Porto, Rua Dr. Roberto Frias, 4200-465 Porto, Portugal; rnatal@fe.up.pt

International Journal of Microwave Science and Technology

Special Issue on CMOS Application to Wireless Communications

Call for Papers

Recent advances in semiconductor process technologies have motivated the development of fully integrated CMOS circuits for wireless communications. Consequently, tremendous research efforts have been directed to the design and implementation of CMOS radio-frequency integrated circuits (RFICs). The objective of this special issue is to highlight the up-to-date progress in the field of CMOS RF devices and circuits.

The International Journal of Microwave Science and Technology invites authors to submit papers for the special issue on CMOS RF. Original papers previously unpublished and not currently under review by another journal are solicited for this special issue. Topics of interest include, but are not limited to:

- CMOS and BiCMOS RF device technologies
- Small-signal circuits
- Large-signal circuits
- Mixed-signal circuits
- Millimeter-wave integrated circuits
- Signal generation circuits
- Frequency-conversion circuits
- Wide-band integrated circuits
- Cellular system IC's and architecture
- Emerging RF applications
- Modeling and CAD

Before submission, authors should carefully read over the journal's Author Guidelines, which are located at http://www.hindawi.com/journals/ijmst/guidelines.html. Prospective authors should submit an electronic copy of their complete manuscript through the journal Manuscript Tracking System at http://mts.hindawi.com/, according to the following timetable:

Manuscript Due	September 1, 2009
First Round of Reviews	December 1, 2009
Publication Date	March 1, 2010

Lead Guest Editor

Liang-Hung Lu, Department of Electrical Engineering, National Taiwan University, Roosevelt Road, Taipei 106, Taiwan; lhlu@cc.ee.ntu.edu.tw

Guest Editor

Huei Wang, Department of Electrical Engineering, National Taiwan University, Roosevelt Road, Taipei 106, Taiwan; hueiwang@ntu.edu.tw

EURASIP Journal on Image and Video Processing

Special Issue on Fast and Robust Methods for Multiple-View Vision

Call for Papers

Image and video processing has always been a hot research topic, and has many practical applications in areas such as television/movie production, augmented reality, medical visualization, and communication. Very often, multiple cameras are employed to capture images and videos of the scene at distinct viewpoints. In order to efficiently and effectively process such a large volume of images and videos, novel multiple-view image and video processing techniques should be developed.

The classical problem of multiple-view vision has been studied by a lot of researchers over the past few decades, and numerous solutions have been proposed to tackle the problem under various assumptions and constraints. Early methods developed in the 1980s and 1990s have laid down the foundations and theories for resolving the multiple-view vision problem. Nonetheless, many of these methods lack robustness and work well only under a well-controlled scene (e.g., homogeneous lighting, wide-baseline viewpoints, texture-rich surface).

Recently, a number of researchers revisit the multiple-view vision problem. Based on the well-developed theories on multiple-view geometry, they adopt robust implementations like statistical methods to produce solutions that can work well under general scene settings. Despite their robustness, these methods are often extremely computationally expensive and require days or even weeks to run and produce results. Therefore, efficient algorithms and implementations will be required to make those methods more practical. Techniques that are developed in real-time image/video processing can be redesigned and adapted for this interesting scenario.

This special issue targets at striking a balance between the efficiency and robustness of methods for multiple-view vision. This helps to bring multiple-view methods from laboratories to general home users. Topics of interest include, but are not limited to:

- Fast and robust feature detection and description
- Fast and robust feature matching and tracking
- Fast and robust camera calibration
- Efficient and precise image segmentation and registration
- Real-time 3D reconstruction/modeling
- Real-time texture and motion recovery
- Real-time robot navigation of dynamic scenes
- Multiview recognition algorithms
- Multiview vision algorithms for medical applications
- Stereo and multiview vision for 3D display and projection techniques
- Multiview image and geometry processing for 3D cinematography
- Compression and transmission of multiview video streams
- 3D video synchronization and optical modeling
- Video-based rendering in dynamic scenes
- Distributed and embedded algorithms for real-time geometry and video processing

Before submission, authors should carefully read over the journal's Author Guidelines, which are located at http://www.hindawi.com/journals/ivp/guidelines.html. Prospective authors should submit an electronic copy of their complete manuscripts through the journal Manuscript Tracking System at http://mts.hindawi.com/, according to the following timetable:

Manuscript Due	August 1, 2009
First Round of Reviews	November 1, 2009
Publication Date	February 1, 2010

Lead Guest Editor

Ling Shao, Philips Research Laboratories, 5656 AE Eindhoven, The Netherlands; l.shao@philips.com

Guest Editors

Amy Hui Zhang, United International College, Zhuhai, 519085 Guangdong, China; amyzhang@uic.edu.hk

Kenneth K. Y. Wong, Department of Computer Science, The University of Hong Kong, Hong Kong; kykwong@cs.hku.hk

Jiebo Luo, Kodak Research Laboratories, Rochester, NY 14650, USA; jiebo.luo@kodak.com